Effect of Density Homogeneity on the Dynamic Response of Powder Beds

T. Yanagida and A. J. Matchett
Dept. of Chemical Engineering, School of Science and Technology, University of Teesside, Middlesbrough, TS1 3BA, U.K.

J. M. Coulthard
Dept. of Civil Engineering, School of Science and Technology, University of Teesside, Middlesbrough, TS1 3BA, U.K.

B. N. Asmar, P. A. Langston, and J. K. Walters
School of Chemical, Environmental and Mining Engineering, University of Nottingham, University Park, Nottingham, NG7 2RD, U.K.

Homogeneous and inhomogeneous powder beds subjected to low-magnitude vibration are compared in terms of the dynamic response. The inhomogeneous samples were segregated into two phases: loose and dense phases, layering the two phases horizontally or vertically. An apparent mass, defined as a ratio of the base force to base acceleration, was measured. Comparison of homogeneous and segregated data demonstrated a significant density gradient dependence on the apparent mass data. First, homogeneous systems showed a resonant peak, which gave the longitudinal elastic modulus of the bed via the velocity of longitudinal stress wave propagation. Second, vertically segregated systems exhibited two significant peaks at low frequencies, corresponding to the resonance of each phase. In addition, the apparent mass values at the two peaks were related to the quantity of each phase. Third, horizontally segregated systems exhibited a resonant peak, whose frequency was approximately equal to homogeneous data, but the apparent mass value at the peak differed from homogeneous data. A model based on the fourth-power scaling law, two-phase theory and Rayleigh's energy method gave an interpretation for the insensitivity of the peak frequency to the density gradient in the vertical direction.

Introduction

The properties and quality of particulate products are dependent upon the means of processing (He et al., 1996; Lu et al., 2000; Yeh et al., 1988; Zhao et al., 1988). To ensure excellence and consistency in the final product, an understanding of the dynamic properties is desired throughout the various processing stages. The dynamic response and properties of powders have been known to be inherently dependent upon the particle packing state (Bika et al., 2001; Das, 1993; Fayed et al., 1997; Shinohara et al., 2000; Yanagida et al., 2002).

Correspondence concerning this article should be addressed to A. J. Matchett.

Measurements of the dynamic response give elastic information for powder assemblies. Mechanical properties of powders and bulk solids are often characterized by rigid-plastic models, where elastic effects are ignored (Fayed et al., 1997; McGlinchey et al., 1997). However, a knowledge of the elastic regime is essential to a complete model of bed behavior, and systems must pass through the elastic region in order to deform plastically. It also has been shown that the elastic modulus can be related to packing conditions (Kendall et al., 1987; Yanagida et al., 2002c), and also to the quality of mixing in a two-component system (Yanagida et al., 2002a,b).

This study investigates the effect of density homogeneity upon the dynamic response of powder beds subjected to low-magnitude vibration. Variations in packing can have a detrimental effect upon properties in agglomerates, compacts, and tablets. Areas of low solids density can cause structural weakness. Likewise, areas of high density can cause stress localization upon stress relaxation, leading to a breakdown of the structure.

As to the particle packing dependence upon the dynamic properties, Kendall et al. (1987) investigated theoretically and experimentally the effect of packing fraction upon the elasticity of particle assemblies. Their theory appeared to describe successfully the experimental values of elastic modulus for particle assemblies, and in particular the strong influence of particle packing, which was theoretically predicted to be the fourth power of solid volume-packing fraction. Trappe et al. (2001) studied a phase transition from fluidlike to solidlike weakly attractive colloidal particles by measuring the viscosity and elastic modulus, reporting that the elastic modulus conformed to the fourth-power scaling law. Similar scaling laws have also been reported (Arato et al., 1995; Carneim and Green, 2001; Grant and Russel, 1993).

The transmission of low-magnitude vibration through a shallow powder bed has been shown to be feasible for characterizing the dynamic properties (Alsop et al., 1995, 1997; Matchett and Alsop, 1995; Matchett et al., 1998, 1999, 2000; Okudaira et al., 1994; Okudaira, 1997; Yanagida et al., 2001, 2002). Principally, the method requires a top-cap mass on the bed surface, requiring a preconsolidation of the samples to support the top-cap mass prior to the measurement. This resulted in relatively denser beds compared to a natural packed bed. In previous work (Yanagida et al., 2002), we have demonstrated that the use of apparent mass is able to give nondestructively and noninvasively the stiffness of a loosely packed bed without the top-cap mass. However, these experiments were performed for homogeneous systems, and the density gradient dependence upon the apparent mass data has not been obvious.

For inhomogeneous powder systems subjected to low-magnitude vibration, the strong particle packing dependence upon the dynamic properties may give a dynamic response dissimilar to homogeneous systems due to the density variation. Initially, a study of inhomogeneous systems composed of two phases: loose and dense phases will give an indication of the viability of using the dynamic response data to study these systems.

This article presents a comparison of homogeneous and inhomogeneous powder beds subjected to low-magnitude vibration (0.196 m/s^2) in terms of the dynamic response. The inhomogeneous samples are segregated into two phases: loose and dense phases, layering the two phases horizontally or vertically. Vibration experiments are performed in an open vessel attached to a vibration source via an impedance head. This method enables the properties of inhomogeneous samples to be measured. An apparent mass, defined as the base force to base acceleration, is measured as a function of frequency. Comparison of homogeneous and segregated data upon the apparent mass data is made over a range of frequencies.

Experimental

Experimental apparatus and procedure

The experimental system developed previously (Yanagida et al., 2002) was used in this study. This system is structurally similar to the Top-Cap Method (Okudaira et al., 1994; Okudaira, 1997; Matchett and Alsop, 1995; Matchett et al., 1998, 1999; Yanagida et al., 2001); however, the principle is different. This system is able to perform without the top-cap mass, allowing the properties of inhomogeneous systems to be measured. Figure 1 illustrates the experimental system. A Perspex cylindrical test cell was mounted on an impedance head

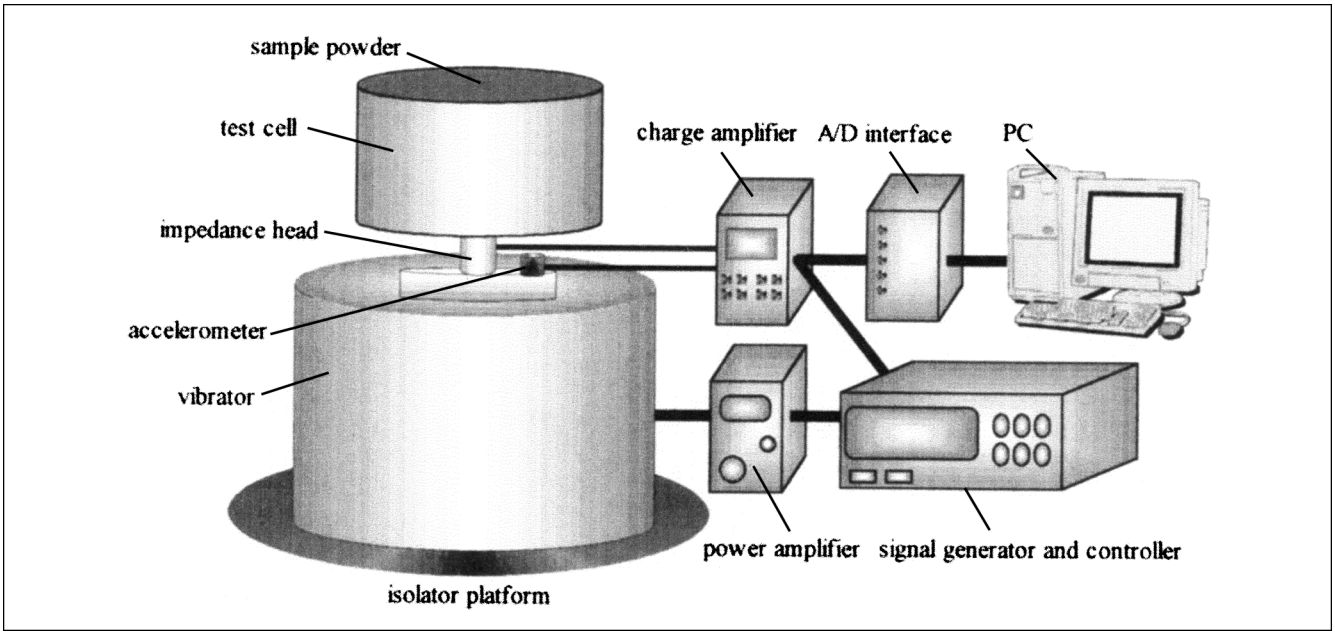

Figure 1. Experimental system developed.

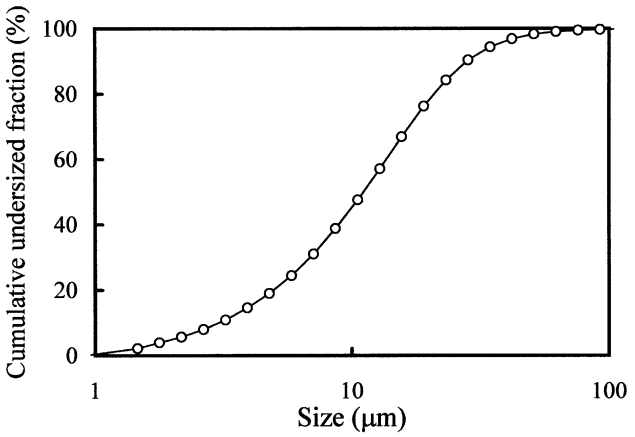

Figure 2. Size distributions of China clay powder used.

(9311B, Kistler), consisting of a force transducer, driven by an electromechanical vibrator (V403, Ling Dynamic Systems), with a vertical line of action. The test cell sizes were ranged from 0.01 to 0.08 m for the vessel height and 0.0345 to 0.149 m for the vessel inner diameter to investigate the effect of the vessel shape. The vibration exciter was placed on an isolator platform to minimize other sources of noise from the general surroundings. Preliminary tests demonstrated that the background noise was found to be negligible within this study. The vibrator was a system with a programmable, feedback controller (DSC4, CED). Feedback control was achieved via the accelerometer (8636C50, Kistler) on the base plate, which provided input signals for the controller to modify and provided output feed to the power amplifier (PA100E, Ling Dynamic Systems), which drove the vibrator, to give a required acceleration at a chosen frequency range. The accelerometer and force transducer were of the piezoelectric type. They were connected via a coupler to an A/D interface (1401, CED), which recorded data at a rate of 12.5 kHz per channel onto the hard disc of a PC. The sampling frequency was larger than the minimum sampling frequency, that is, Nyquist frequency, which was 8 kHz within the range of this study, based upon Shannon's sampling theorem (Norton, 1989). The piezoelectric devices are characterized by very rapid response times with high accuracy and reproducibility, providing very reliable data acquisition.

The sample powders were placed carefully into the test cell by gravity using a spatula, and the surface of the bed was subsequently leveled with a straight edge. Then, a sweep vibration that ranged from 10 Hz to 4,000 Hz was applied to the test cell through the base at a chosen sweep rate of 5 Hz/s with a constant peak acceleration of 0.196 m/s^2. The values of vibrational parameters have been found to be appropriate for measurement (Yanagida et al., 2002). Within this frequency range, the vibrator, force transducer, and accelerometer were precise and independent of their structural resonance.

The level of applied acceleration (0.02 g) was very low and did not cause gross deformation of the powder beds. Particle–particle contacts were maintained with no change in packing conditions or bulk density. This has been confirmed many times by experimental observation (Yanagida et al., 2002).

During a sweep, data from two measurement devices were monitored as a time series on the hard disk of the computer. The collected data points for each channel were 1.0×10^7. Subsequently, these time-series data were analyzed by FFT, with the sampling number of 4096 points to give the frequency data. An apparent mass, defined as the ratio of base force to base acceleration, was calculated by the computer. To ensure the reproducibility of tests, each test was repeated three times. The deviation upon the bulk density for each test was within $\pm10\%$ over the range of this study.

Sample powders

Experiments were performed on China clay powder (Grade D, ECC international), with the size distribution shown in Figure 2. The size data of clay were measured by a laser diffraction analyzer (MSIZER, Malvern Instruments). The physical properties of the clay powder are given in Table 1 (Lee et al., 1983; Waterman and Ashby, 1997). The loose bulk density was measured by pouring the known weight of the material through a standard funnel into a measuring cylinder. In order to measure the tapped bulk density, this was then compacted by lifting the cylinder and allowing it to drop from a fixed height until no observable change in bulk density occurred.

Inhomogeneous samples composed of two phases

The measurement system enables the properties of inhomogeneous systems to be measured. In this study, horizontally and vertically segregated systems, composed of two phases, were employed. The segregated systems are shown in Figure 3.

The following two tests were carried out for these segregated systems. These tests were repeated three times to ensure the reproducibility.

(1) Constant Two Volume-Packing Fractions Test. In this test, the volume-packing fractions of two phases were set to be constant. The volume fraction of each phase was varied, resulting in changes upon the total volume-packing fraction.

(2) Constant Total Volume-Packing Fraction Test. Tests were performed with the total volume-packing fraction being constant. The combination of the packing fractions of two phases was varied, resulting in different density profiles.

Preparation of segregated samples

Horizontally Segregated Systems. It was possible for horizontally segregated systems to manipulate the volume-packing fraction of each phase by preconsolidation and measuring

Table 1. Physical Properties of Clay Powder Used

	Mean Size (μm)	True Dens. (kg/m^3)	Loosed Bulk Dens. (kg/m^3)	Tapped Bulk Dens. (kg/m^3)	Hausner Ratio
China clay-kaolin	10.5	2,640	367	670	1.826

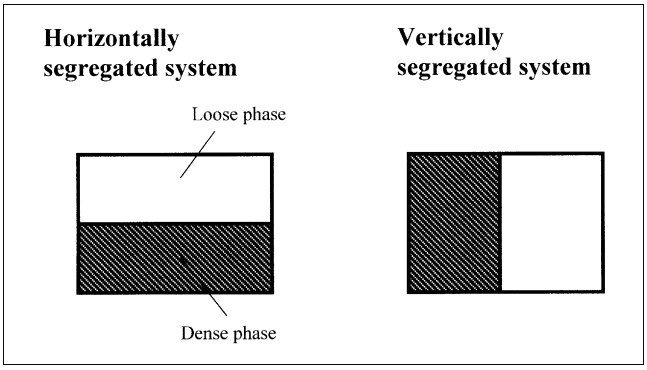

Figure 3. Inhomogeneous segregated systems made.

each bed height. In this study, only the case in which the loose phase was on top was investigated. Experimentally, the alternative case, in which the dense phase was on top, was not feasible because the bottom phase was easily consolidated due to the addition of the top phase.

Powders with a known mass were poured into the sample cell, and subsequently tapped by vertical vibration of 50 Hz and 2 g. The preconsolidation was performed until the bed height reached a desired value for the dense phase, h_D, which is given by

$$h_D = \frac{m_D}{A\phi_D\rho_p} \tag{1}$$

where A is the cross-sectional area of phase, m_D is the mass of dense phase, ϕ_D is the volume-packing fraction of the dense phase, and ρ_p is the true density of material.

After preparation of the dense phase, powders for the loose phase were carefully poured into the sample cell on top of the dense phase. For horizontally segregated systems, the volume fraction of the dense phase can be represented by the fraction of the bed height. For constant two volume-packing fractions tests, the fraction was varied from 0 to 1, while for constant total volume fraction tests, the fraction was set to be a constant value—0.5.

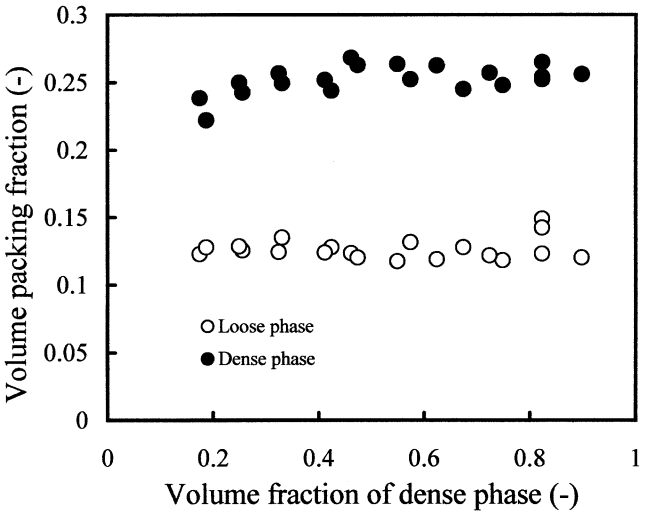

Figure 4. Volume-packing fractions of two phases of horizontally segregated systems.

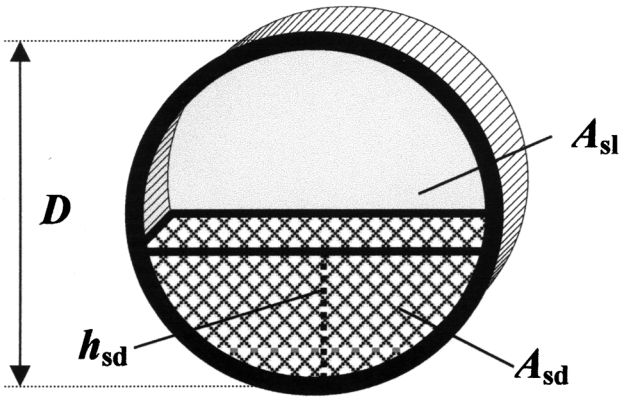

Figure 5. Geometrical shape of the dense phase consolidated for vertically segregated systems in cylindrical test cell.

Figure 4 shows typical data of the volume-packing fractions of two phases, which was made for constant two volume-packing fractions tests. There were variations on the volume-packing fractions, and data were ranged within ± 0.02 from the mean value.

Vertically Segregated Systems. Powders with a known mass were poured into the cell, and the test cell was rotated vertically through 90 degrees. A flat board was set to seal the material in the cell and prevent samples from flowing out. The cell was then tapped by vibration of a vertical line of action. Subsequently, powders for the loose phase were poured into the rest of vessel space using a spatula, and leveling the bed surface as necessary with a straight edge. Since the vessel was a cylindrical shape, the phase volume was estimated by the following manner.

The tapped powders were found to be crescent-shaped, as seen in Figure 5. Obviously, the area gives the value of the phase volume. Let h_{sd} be the maximum bed depth from the vessel wall, which is measurable. The area of the dense phase, A_{sd}, is given from a geometrical relationship as follows

$$A_{sd} = \left[\frac{D^2}{4}\cos^{-1}\left(1-\frac{2h_{sd}}{D}\right)\right] - \left\{\frac{D}{2}\left(\frac{D}{2}-h_{sd}\right)\sin\left[\cos^{-1}\left(1-\frac{2h_{sd}}{D}\right)\right]\right\} \tag{2}$$

where D is the diameter of the vessel.

Also, the area of loose phase, A_{sl}, is

$$A_{sl} = \frac{\pi D^2}{4} - A_{sd} \tag{3}$$

Consequently, measuring h_{sd} gives the value of each phase volume. By determining the desired value of h_{sd} for each experimental configuration prior to preconsolidation, the packing state of the dense phase was controlled.

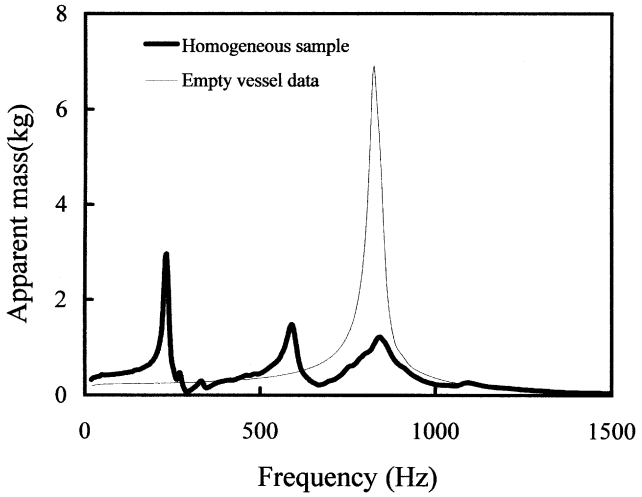

Figure 6. Typical apparent mass data of homogeneous samples.

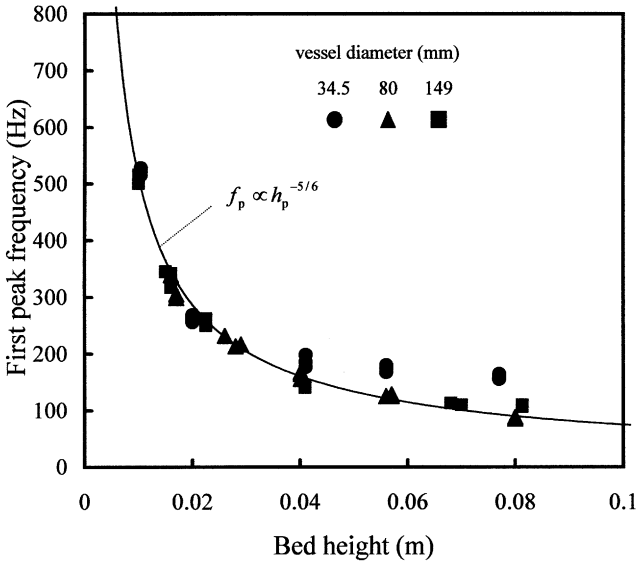

Figure 7. Effect of vessel dimension upon the first peak frequency.

Results and Discussion

Apparent mass data of homogeneous samples

Figure 6 shows typical apparent mass data of homogeneous samples along with data of the empty vessel. The vessel dimensions were 0.149 m inner diameter and 0.04 m height, and the vessel resonance was found to be around 800 Hz. It can be seen that the presence of powder beds exhibited a significant peak around 200 Hz. In such low-frequency ranges, it is obvious that the vessel acts as a good approximation to a rigid body, indicating that the peak exhibited by powders could be due to the bed resonance. Furthermore, a second peak was seen around 550–600 Hz. The second peak frequency was found to be nearly three times of the first peak frequency, in agreement with the theory for the one-end-fixed vibration mode (Norton, 1989). Figure 7 shows the effect of vessel dimension upon the first peak frequency. The peak frequency decreased with increasing bed height, and was approximately proportional to the power of $-5/6$ of the bed height, predicted by Hertzian contacts. A discrepancy between different vessel diameters was found for deep beds, indicating wall effects. For shallow beds below 0.04 m of the bed height, the peak frequency was found to be insensitive to the vessel diameter, but dependent only on the bed height. This allows us to use the shallow-bed system without wall effects showing any significant contribution. In the following experiments, a vessel dimension with a diameter of 0.149 m and a bed height of 0.04 m was used, that is, the aspect ratio was 0.268.

The measured peak frequency gives the longitudinal elastic modulus of the bed as follows (Yanagida et al., 2002). Here, we consider the bed dynamics in the longitudinal direction. Since the mode shape is considered to be the one-end-fixed longitudinal vibration mode, the velocity of the longitudinal stress wave propagation through the bed, v_p, is given in terms of the peak frequency, f_p, and the bed height, h_p, as follows (Das, 1993; Okudaira et al., 1993)

$$v_p = 4h_p f_p \tag{4}$$

If v_p is expressed as $\sqrt{Y/\rho_b}$ (ρ_b is the bulk density of the bed), then Y is given by

$$Y = \rho_b (4h_p f_p)^2 \tag{5}$$

Consequently, Eqs. 4 and 5 enable Y and v_p to be quantified from the measured f_p along with h_p and ρ_b, which are also experimentally measurable. Table 2 shows the calculated data of Y and v_p with the packing fraction. For comparison, data generated by the Top-Cap Method with a top-cap mass of 0.096 kg (Okudaira et al., 1994; Okudaira, 1997) are shown in the table. The sample powder was preconsolidated to support the top cap. Clearly, a substantial discrepancy was found with the packing fraction change.

Kendall et al. (1987) considered the ensemble elastic modulus of a particle assembly to be dependent on the contacts between individual particles, and proposed the following mathematical relationship between the effective elastic modulus, Y, the material elastic modulus, Y_t, the interfacial energy of the solid particles, Γ, the volume-packing fraction of solids, ϕ_T, and the particle diameter, d_p

$$Y = 17.1\phi_T^4 \left[\frac{\Gamma Y_t^2}{d_p}\right]^{1/3} \tag{6}$$

The formula implies the very strong influence of particle packing through the fourth-order relationship. Furthermore, Kendall et al. (1987) demonstrated that the fourth-power scaling law was applicable for titania, zirconia, silica, and alumina powders whose particle sizes were submicron.

Table 2. Y and v_p Estimated from the Peak Frequency

	Y (Pa)	v_p (m/s)	ϕ
Present measurement	2.51×10^5	26.4	0.137
Top-cap method	8.93×10^5		0.196

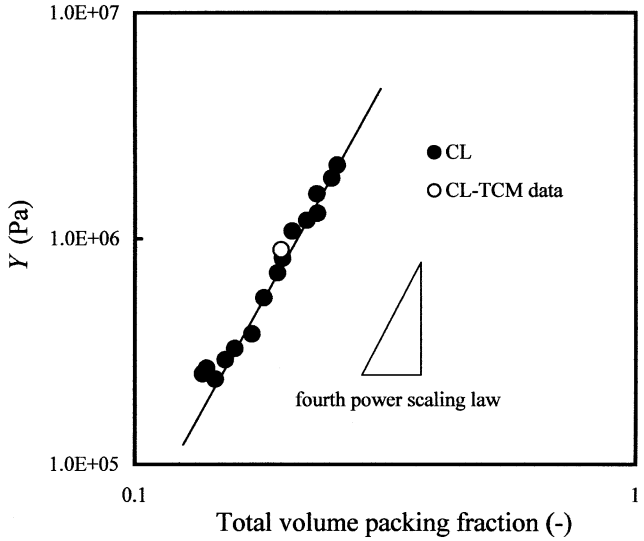

Figure 8. Longitudinal elastic modulus *Y* as a function of total volume-packing fraction.

In order to manipulate the packing condition, vibration and compaction by a 1.59-kg iron disk were adopted. The applied vibration was 50 Hz, and the acceleration levels ranged from 1 g to 3 g. After pouring a known weight of samples into the test cell, the preconsolidation was performed until no observable change in bulk density occurred. This was repeated until the samples filled the test cell, and the bed surface was leveled with a straight edge as necessary. The preconsolidation was carried out carefully to ensure a homogeneous mass distribution within the bed. Figure 8 shows Y as a function of the total volume-packing fraction. The results gave a reasonable agreement to the fourth-power scaling law over a range of packing fraction, including a natural packed bed. In addition, the Top-Cap Method data were consistent with the data of preconsolidated samples for an identical packing fraction. This is consistent with previous data (Yanagida et al., 2002).

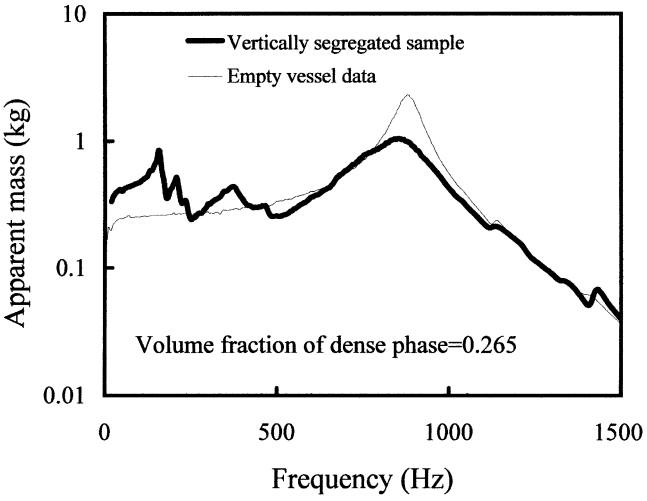

Figure 9. Typical apparent mass data of vertically segregated systems.

These results highlight that a measure of apparent mass data is capable of determining the properties of loosely packed powder beds, which has not been possible using the Top-Cap Method or other methods, for example, a three-points bed method and an unconfined compression test (Kendall et al., 1987; Mcglinchey et al., 1997; Richardson et al., 2000).

Apparent mass data of inhomogeneous samples

The preceding results revealed the very strong influence of particle packing upon the stiffness through the fourth-order relationship. For inhomogeneous systems subjected to low-magnitude vibration, the strong particle packing dependence may result in a dynamic response dissimilar to homogeneous systems, due to the density variation. In this section, the effect of density homogeneity upon the apparent mass data is examined by using horizontally and vertically segregated samples, which are comprised of two phases.

Vertically segregated systems

The following experiments were performed with volume-packing fractions of two phases, which were set to be constant, changing the volume fraction of each phase. Figure 9 shows typical apparent mass data of vertically segregated systems. The volume fraction of the dense phase was 0.265. The volume-packing fractions of the dense and loose phases were set to be 0.19 and 0.12, respectively. Below 300 Hz, the vertical segregated system exhibited two significant peaks. The two peaks were observed over the range of the dense-phase volume fraction. Clearly, this differs from the homogeneous data, which showed a single peak corresponding to the bed resonance. Furthermore, the frequency values of the two peaks were found to be insensitive to the volume fraction of the dense phase (Figure 10), regardless of the fact that the total volume-packing fraction was increased by increasing the volume fraction of the dense phase. This infers that the two phases excite harmonic resonance, resulting in the two reso-

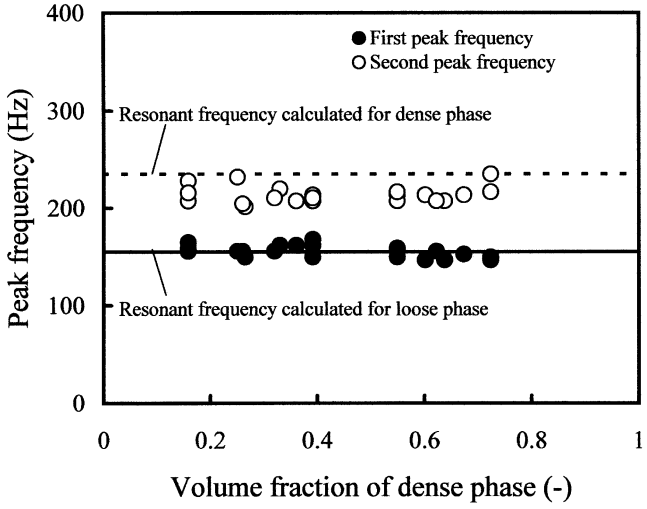

Figure 10. Peak frequencies of vertically segregated systems as a function of the volume fraction of the dense phase.

nant peaks. Above 300 Hz, data exhibited several peaks, and their trends were found to be complex. Presumably, the higher vibration modes of each phase, the interaction effects between two phases, the effect of vessel resonance, and other mechanisms might be related to those trends. Although further study needs to be undertaken to understand the nature of these trends, the following discussion will deal with the data of the two peaks below 300 Hz.

Homogeneous data in the section titled "Apparent mass data of homogeneous samples" enables the resonant frequencies of two phases to be estimated in terms of the fourth-power scaling law calculated as separate homogeneous beds (Figure 10). The calculated data gave a reasonable agreement to experimental data, specifically for the first peak. The second peak deviated somewhat from the data for the dense phase. Statistical analysis (t-test) demonstrated that there was a significant difference between the second peak and the resonant frequency calculated for the dense phase at the 0.05 level of significance—$|t_0| = 10.81 > t(20,0.05)$—but not for the first peak—$|t_0| = 0.062 < t(20,0.05)$. However, the mean of the second peak was 214 ± 21 Hz, compared with the value calculated for the dense phase (235 Hz).

The value of the second peak frequency is close to, but significantly less than that of an equivalent single bed. The discrepancy may be due to a number of reasons, including: wall effects; interactions between the dense and loose beds; experimental imperfections in preparation of the two beds, it being easier to prepare the loose bed. Further investigations are required in this area.

Figure 11 shows the apparent mass values of the two peaks as a function of the volume fraction of the dense phase. The value at the first peak decreased by increasing the volume fraction of the dense phase, whereas the second peak value increased. Above 0.5 of the volume fraction of the dense phase, the first peak value did not show a significant trend. In such ranges, the second peak tends to be significant, as the volume fraction of the dense phase tends to increase. This results in the increased apparent mass data below the second

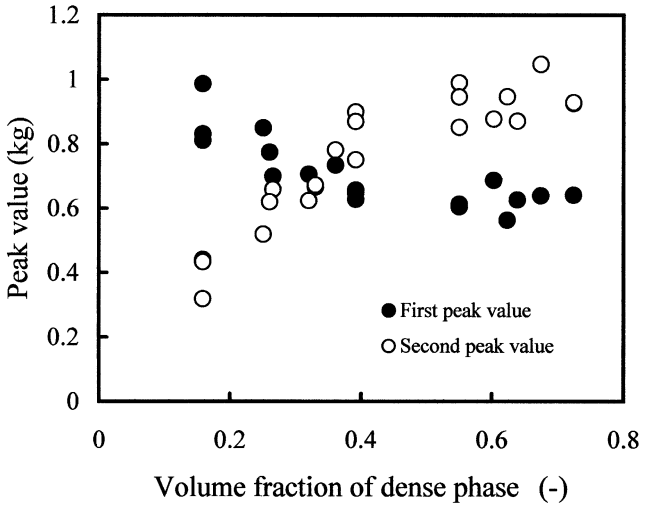

Figure 11. Apparent mass values at the two peaks of vertically segregated systems as a function of the volume fraction of the dense phase.

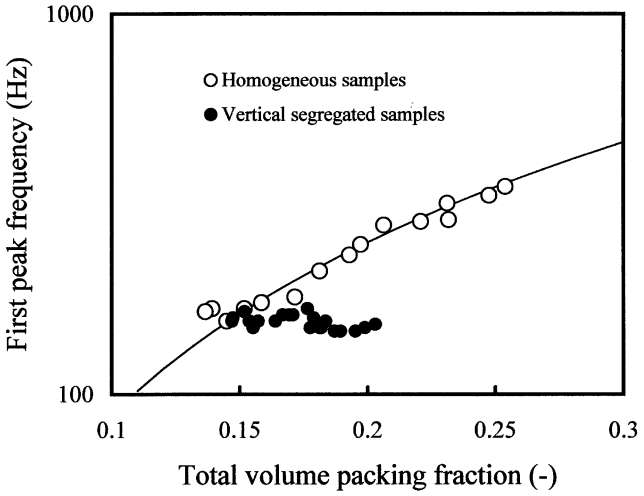

Figure 12. Comparison of vertically segregated and homogeneous systems in terms of the first peak frequency.

peak frequency. Statistical analysis showed (1) the negative correlation between the first peak value and the volume fraction of the dense phase—$r = -0.771$, and (2) the positive correlation for the second peak value ($r = 0.895$). Also, these correlation coefficients were found to be significant at the 0.05 level of significance—$|r| > r(19,0.05) = 0.4329$. The results in Figure 11 show that the apparent mass value at each peak is related to the quantity of each phase.

Figure 12 shows a comparison of vertically segregated and homogeneous systems in terms of the first peak frequency as a function of total volume-packing fraction. According to the fourth-power scaling law, the peak frequency should be proportional to 3/2 of power of the total volume-packing fraction. Although homogeneous data conformed to the scaling law, vertically segregated data showed insensitivity to the total volume-packing fraction. This is consistent with the preceding implication that the first peak frequency of vertically segregated systems relies on the resonance of loose phase, that is, the packing state, which was experimentally controlled to be almost constant.

The results in this section revealed that:

- Vertically segregated systems, made up of two phases, exhibit two significant peaks on the apparent mass data at low frequencies, showing a clear difference to homogeneous data, which showed a single peak corresponding to the bed resonance;
- The two peaks are caused by the resonance of each phase as though acting independently, and the peak frequencies are approximately predictable in terms of the fourth-power scaling law along with homogeneous data;
- The peak value is related to the quantity of each phase;
- Consequently, measuring the apparent mass may give useful information regarding the density gradients in the horizontal direction.

Further works need to be undertaken, however, to confirm the feasibility of this method for a wide range of inhomogeneous situations, since this study has dealt with only the simplest case composed of two phases.

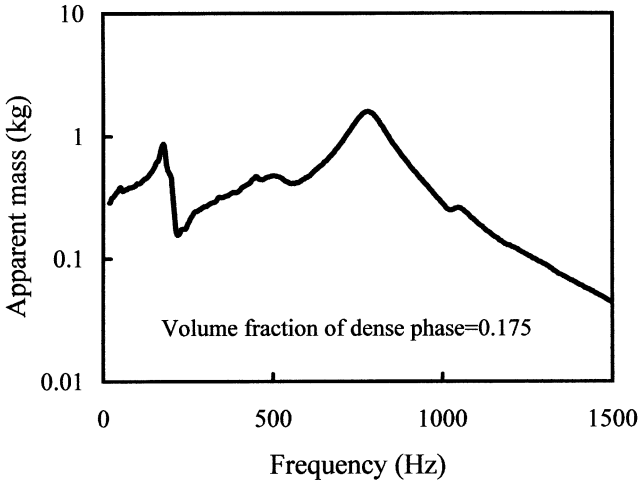

Figure 13. Typical apparent mass data of horizontally segregated systems.

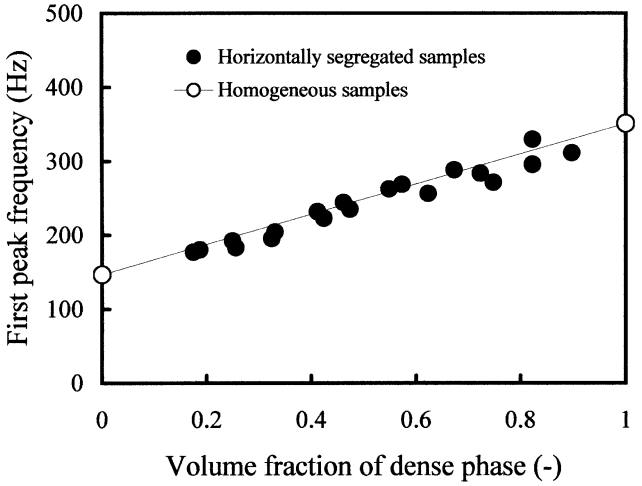

Figure 14. First peak frequency of horizontally segregated systems as a function of the volume fraction of the dense phase with volume-packing fractions of two phases being constant.

Horizontally segregated systems

Horizontally segregated systems are now examined by measuring the apparent mass data. Experiments were performed with volume-packing fractions of two phases, set to be constant, changing the volume fraction of each phase. The volume-packing fractions of loose and dense phases were set to be 0.12 and 0.25, respectively.

Figure 13 shows typical apparent mass data of horizontally segregated systems. The data exhibited a peak at low frequencies below 300 Hz. This was also found to be significant over the volume fraction range of the dense phase. The result is similar to the homogeneous data in spite of the difference of the density gradient in the vertical direction. Two significant peaks above 300 Hz were found. The shape peak of around 800 Hz is excited due to the vessel resonance. The other peak may be related to higher vibration modes. The relationship between the measured first peak and the homogeneity of horizontally segregated systems will be discussed in the following discussion.

Figure 14 shows the first peak frequency as a function of the volume fraction of the dense phase. In contrast to vertical segregated systems, the first peak frequency was found to be sensitive to the volume fraction of the dense phase, that is, the total volume-packing fraction. The data increased linearly when the volume fraction of the dense phase was increased within the limiting values of the resonant frequencies of the two phases. Hence, the first peak frequency of a horizontally segregated system can be calculated by the volume-weighted average of the values for uniform systems of the same depth.

Figure 15 shows a comparison of horizontally segregated and homogeneous systems in terms of the first peak frequency as a function of the total volume-packing fraction. The horizontally segregated data were found to be approximately equal to the homogeneous data. This implies that the peak frequency is almost insensitive to the density gradients in the vertical direction for the horizontally segregated systems used. The nature of the peak frequency of the horizontally segregated systems would be related to the resonance of both phases and its interaction effects. Figure 16 shows a comparison of resonant frequencies of the two phases, predicted by the fourth-power scaling law, and the experimental first peak frequency. Below 0.6 of the volume fraction of the dense phase, the experimental peak frequency agreed reasonably well with the resonant frequency calculated for the loose phase, indicating the dominance of the loose-phase resonance on the first peak. In such ranges, the calculated data for the dense phase were predicted to be much higher than the experimental data, demonstrating the small effect of the dense phase on the first peak. Above 0.6, experimental data began to deviate from the data calculated for the loose phase, and a significant discrepancy between the calculated data and experimental data was seen. Consequently, unlike vertically segregated systems, the nature of horizontally segregated sys-

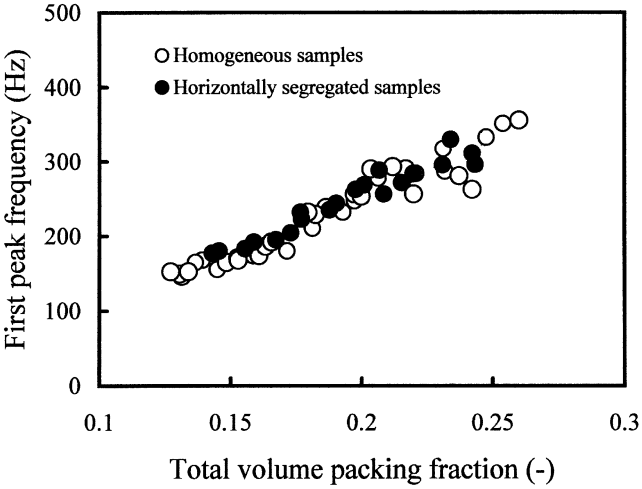

Figure 15. Comparison of horizontally segregated and homogeneous systems in terms of the first peak frequency.

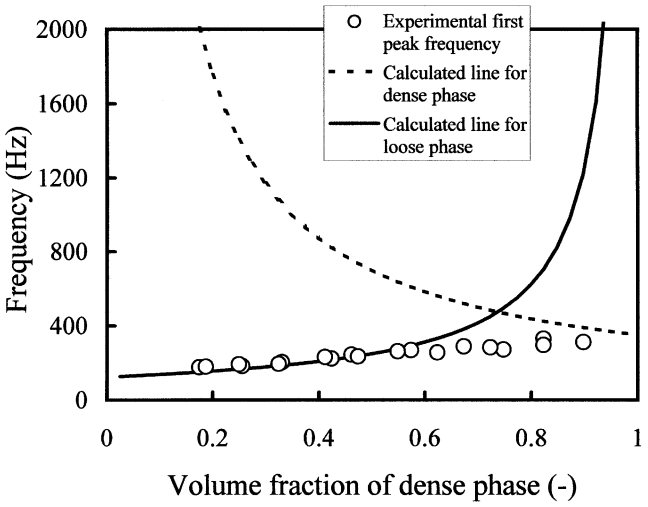

Figure 16. Comparison of the first peak frequency of horizontally segregated systems and resonant frequencies calculated for two phases using the fourth-power scaling low along with homogeneous data.

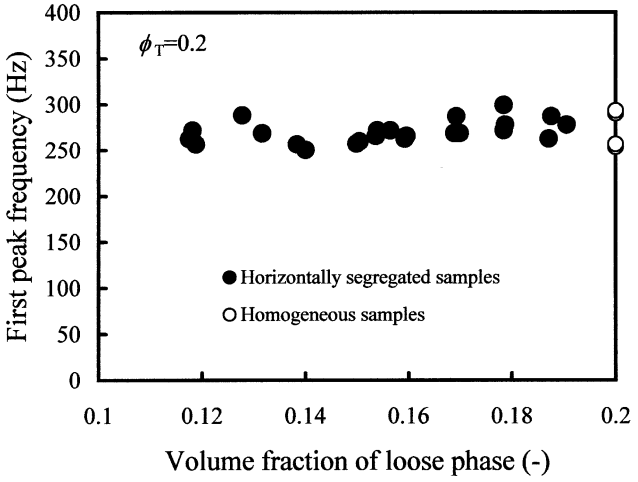

Figure 18. First peak frequency of horizontally segregated systems as a function of the volume-packing fraction of the loose phase with total volume-packing fraction being constant.

tems cannot be simply explained in terms of the resonance of the two phases. Furthermore, the volume-weighted averaging rule of uniform beds of the same depth can be clearly seen in Figure 16.

Figure 17 shows the values of the apparent mass data at the first peak as a function of the total volume-packing fraction, along with homogeneous data. There appeared to be a significant difference between segregated and homogeneous data in the peak values. The homogeneous data increased almost linearly when the total volume-packing fraction on the log-log plot increased, whereas the segregated data were found to be approximately constant below 0.2 of the total volume-packing fraction, and then rapidly increased. Interestingly, the inflection point on the segregated data corresponds to the point on Figure 16, in which the experimental peak frequency began to show significant deviations from the resonant frequency calculated for the loose phase. Presumably, the peak value can be related to the amplitude profile within the beds. When the loose phase dominates the first peak, the dense phase acts almost as a rigid body, resulting in the small effects of the dense phase upon the first peak data. Consequently, such situations may exhibit small apparent mass data because of the light mass of the loose phase. Once the dense phase dominates the peak, the apparent mass may increase when the volume fraction of the dense phase increases, that is, increasing the total volume-packing fraction.

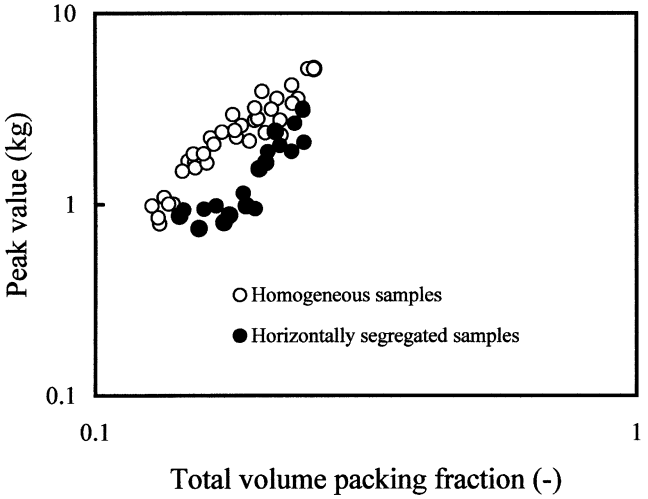

Figure 17. Value of apparent mass at the first peak of horizontally segregated systems as a function of the volume fraction of the dense phase.

The preceding results showed the insensitivity of the first peak frequency to the density gradient in the vertical direction. However, those experiments were performed with the volume-packing fractions of two phases, which were set to be constant. Consequently, it is interesting to investigate segregated samples composed of various volume-packing fractions, with the total volume-packing fraction being constant.

Experiments were performed with a constant total volume-packing fraction of 0.2, changing each packing fraction of two phases. The details of the experimental configurations were shown in the section titled "Preparation of segregated samples." Figure 18 shows the first peak frequency as a function of the loose phase packing fraction. Data of homogeneous samples are shown in the figure for comparison. The insensitivity of the first peak frequency was found to be significant for various packing fractions of two phases. To understand the nature of horizontally segregated systems, it would be necessary to consider several factors, such as the amplitude profile within beds, the interaction between two phases, and the height dependence of phase stiffness. A model incorporating such factors will be developed in next section.

A model for horizontally segregated systems

A model based on the fourth power scaling law, two-phase theory, and Rayleigh's energy method is presented to understand the nature of horizontally segregated systems.

Consider a two-phase bed equivalent to the horizontal segregated system.

Here, we use the following notations in the model: A is the cross-sectional area of phase, h is the height of phase, k is the stiffness of phase, m is the mass of phase, β is the coefficient of the fourth-power scaling law, ϕ is the volume-packing fraction of phase, ρ_p is the true density of material. Let subscripts L, D, and T refer to loose, dense, and total phases, respectively.

Adapting the fourth-power scaling law, the stiffness of each phase is given as

$$k_L = \frac{\beta \phi_L^4 A}{h_L} \tag{7}$$

$$k_D = \frac{\beta \phi_D^4 A}{h_D} \tag{8}$$

$$k_T = \frac{\beta \phi_T^4 A}{h_p} \tag{9}$$

Note that Eq. 9 is applicable for a homogeneous bed only.

From the mass balance

$$h_T \phi_T = h_L \phi_L + h_D \phi_D \tag{10}$$

$$h_p = h_L + h_D \tag{11}$$

The simplified two-phase series model (Yanagida et al., 2001) gives the total stiffness k'_T in terms of the stiffness of each phase as follows

$$\frac{1}{k'_T} = \frac{1}{k_L} + \frac{1}{k_D} = \frac{1}{A\beta}\left(\frac{h_L}{\phi_L^4} + \frac{h_D}{\phi_D^4}\right) \tag{12}$$

The stiffness of the layered bed, given by Eq. 12, is not the same as that of a uniform bed of the same average volume fraction solids—Eq. 9. This is apparently contrary to the reported data in Figure 18, and this apparent contradiction will be considered in more detail below.

Rayleigh's energy method (James et al., 1993; Thomson, 1972; Timoshenko et al., 1974) can be used to estimate the effective mass and extended for the horizontally segregated system (Yanagida et al., 2002). The effective mass of segregated system m_1 is given by (see Appendix)

$$m_1 = \frac{m_L(\alpha^2 + \alpha + 1)}{3} + \frac{m_D \alpha^2}{3} = \frac{A\rho_p}{3}\left[h_L \phi_L (\alpha^2 + \alpha + 1) + h_D \phi_D \alpha^2\right] \tag{13}$$

where α is defined as the ratio of the interface amplitude to the bed surface amplitude.

Here α for this model is expressed as (see the Appendix)

$$\alpha = \frac{\phi_L^4 h_D}{\phi_L^4 h_D + \phi_D^4 h_L} \tag{14}$$

Simply, the resonant frequency of total phase f_T is

$$f_T = \frac{1}{2\pi}\sqrt{\frac{k'_T}{m_1}} \tag{15}$$

The formula neglects the damping effects on the resonant frequency, which has been shown to be reasonable within this study (Yanagida et al., 2001, 2002).

Equations 12–15 can be used to calculate the resonant frequency. The calculation requires values of A, h_D, h_L, β, ϕ_D, ϕ_L, and ρ_P, which are experimentally measurable. Consequently, this model can be implemented by the known physical properties of each phase without any arbitrary fitted parameters.

Let us examine the effect of density homogeneity on the resonant frequency of horizontally segregated systems using the preceding model. Here, we consider the situations where the volume-packing fractions of the two phases are constant and the dense phase is always at the bottom. The following values equivalent to the experimental configurations are used for the computation

$$h_D = 0.02\ (\mathrm{m}),\quad h_L = 0.02\ (\mathrm{m}),\quad h_T = 0.04\ (\mathrm{m}),\quad \phi_T = 0.2,$$
$$\rho_p = 2{,}640\ (\mathrm{kg/m^3}),\quad A = 1.14\times 10^2\ (\mathrm{m^2}),$$
$$\beta = 5.0\times 10^8\ (\mathrm{Pa})$$

The value of β was determined from homogeneous data.

Figure 19 shows the comparison of the model calculation and experimental data in terms of the first peak frequency as

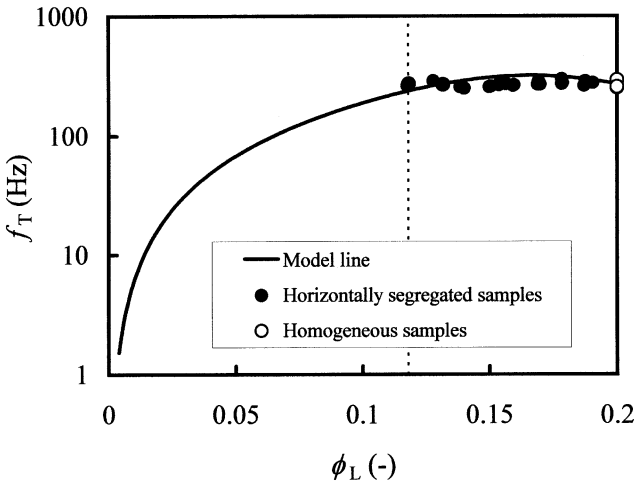

Figure 19. Comparison of the model and experimental data in the first peak frequency as a function of the volume-packing fraction of the loose phase.

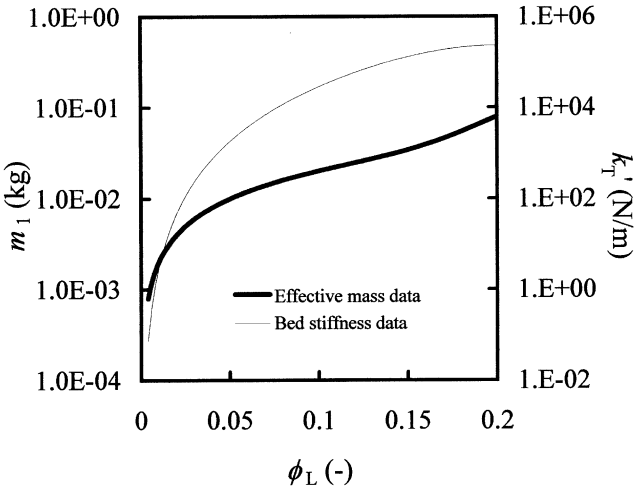

Figure 20. Calculated data of the bed stiffness and the effective mass.

a function of the volume-packing fraction of the loose phase. The broken line in the figure represents the loose volume-packing fraction as an experimental limit, since experimentally the packing fractions, which were lower than the limit, were not possible to make. Unfortunately, under these experimental conditions, the major changes in the first peak frequency with the packing fraction take place below this limit.

Figure 20 shows the effective mass and the bed stiffness data as a function of the volume-packing fraction of the loose phase. In the region of the loose packing fraction, both data decreased when the volume-packing fraction of the loose phase decreased. Combinations of these data allow us to use Eq. 15 to predict the first peak frequency. These data show (Figure 19) a maximum in the range of experimental interest, which is not visible in the experimental data. However, changes in the value of the first peak frequency are relatively small in this region, and the experimental data are in overall good agreement with the model. Thus, both model and experimental data show the relative insensitivity of the first peak frequency to the volume fraction of the loose phase.

Conclusions

The effect of density homogeneity upon the apparent mass data of powder beds subjected to low-magnitude vibration was examined in terms of a comparison of homogeneous and segregated data. The results yielded the following implications:

(1) Homogeneous systems acted as harmonic resonators, showing significant resonant peaks;

(2) The first peak frequency gave the longitudinal elastic modulus of the bed via the velocity of longitudinal stress wave propagation, in good agreement with data generated by the Top-Cap Method;

(3) The particle packing dependence of homogeneous systems conformed to the fourth-power scaling law;

(4) Vertically segregated systems exhibited two significant peaks on the apparent mass data below 300 Hz, indicating a clear difference to the homogeneous data;

(5) The two peaks were caused by the resonance of each phase, as though acting independently, and the peak frequencies were approximately predictable in terms of the fourth-power scaling law along with homogeneous data;

(6) The peak value was found to be related to the quantity of each phase;

(7) Horizontally, the segregated systems showed a peak, whose frequency was almost equal to the homogeneous data for the identical total volume-packing fraction;

(8) The peak frequency was found to be insensitive to the density homogeneity in the vertical direction over a range of volume-packing fractions of two phases within this study;

(9) The apparent mass value at the peak, however, showed a significant difference from the homogeneous data;

(10) In contrast to the vertical segregated data, the resonant frequency data of the two phases, calculated by the fourth-power scaling law, could not give a rigorous interpretation of the nature of the horizontally segregated systems;

(11) A model was proposed based upon the fourth-power scaling law, two-phase theory, and Rayleigh's energy method;

(12) The model gave an interpretation for the nature of the horizontally segregated systems;

(13) The insensitivity of the peak frequency to homogeneity in the vertical direction could be interpreted in terms of similar packing dependencies of both the bed stiffness and the amplitude profile.

The preceding implications indicate that a measure of the apparent mass may give nondestructively intimate information regarding the density profile within the beds. However, further work needs to be undertaken to confirm the feasibility of this method for various inhomogeneous situations, since this study dealt with only the simplest case made up of two phases.

Acknowledgments

The authors thank the Engineering and Physical Sciences Research Council of Great Britain for funding and a collaborative research grant funded by ORS Awards.

Literature Cited

Alsop, S., A. J. Matchett, and J. M. Coulthard, "Experimental Investigation of Effects of Vibration Upon Elastic and Cohesive Properties of Beds of Wet Sand," *Shock Vib. J.*, **2**, 383 (1995).

Alsop, S., A. J. Matchett, J. M. Coulthard, and J. Peace, "Elastic and Cohesive Properties of Wet Particulate Materials," *Powder Technol.*, **91**, 157 (1997).

Arato, P., E. Besenyei, A. Kele, and F. Weber, "Mechanical-Properties in the Initial-Stage of Sintering," *J. Mater. Sci.*, **30**, 1863 (1995).

Bika, D. G., M. Gentzler, and J. N. Michaels, "Mechanical Properties of Agglomerates," *Powder Technol.*, **117**, 98 (2001).

Carneim, T. J., and D. J. Green, "Mechanical Properties of Dry-Pressed Alumina Green Bodies," *J. Amer. Ceram. Soc.*, **84**, 1405 (2001).

Das, B. M., *Principle of Soil Dynamics*, PWS-KENT, Boston (1993).

Fayed, M. E., and L. Otten, eds., *Handbook of Powder Science and Technology*, Chapman & Hall, New York (1997).

Grant, M. C., and W. B. Russel, "Volume-Fraction Dependence of Elastic Moduli and Transition Temperatures for Colloidal Silica Gels," *Phys. Rev. E*, **47**, 2606 (1993).

He, Y. J., A. J. A. Winnubst, C. D. SagelRansijn, A. J. Burggraaf, and H. Verweij, "Enhanced Mechanical Properties by Grain Boundary Strengthening in Ultra-Fine-Grained TZP Ceramics," *J. Eur. Ceram. Soc.*, **16**, 601 (1996).

Kendall, K., N. Mcn. Alford, and J. D. Birchall, "A New Method for Measuring the Surface Energy of Solids," *Nature*, **325**, 794 (1987a).

Kendall, K., N. Mcn. Alford, and J. D. Birchall, "Elasticity of Particle Assembles as a Measure of the Surface Energy of Solids," *Proc. R. Soc. London*, **A412**, 269 (1987b).

Lee, I. K., W. White, and O. G. Ingles, *Geotechnical Engineering*, Pitman, New York (1983).
Matchett, A. J., and S. Alsop, "A Two-Phase Elastic Model of Vibration in a Bed of Particulates," *Powder Technol.*, **83**, 13 (1995).
Matchett, A. J., Maufauvre, and S. Alsop, "An Elastic Shell Model for Wet Particulate Solids," *Powder Technol.*, **96**, 106 (1998).
Matchett, A. J., T. Yanagida, Y. Okudaira, S. Kobayashi and M. Satoh, "Some Initial Experiments with an Electrically Conducting Powder Under Static and Vibrating Conditions," *Adv. Powder Technol.*, **10**, 51 (1999).
Matchett, A. J., T. Yanagida, Y. Okudaira, and S. Kobayashi, "Vibrating Powder Beds: A Comparison of Experimental and Distinct Element Method Simulated Data," *Powder Technol.*, **107**, 13 (2000).
McGlinchey, D., A. J. Matchett, and J. M. Coulthard, "The Vibratory Unconfined Compression Tester (VUCT) for Cohesive Solids," *Chem. Eng. Res. Des.*, **75**(Pt. A), 271 (1997).
Norton, M. P., *Fundamentals of Noise and Vibration Analysis for Engineers*, Cambridge Univ. Press, Cambridge (1989).
Okudaira, Y., Y. Kurihara, H. Ando, M. Satoh, and K. Miyanami, "Sound Absorption Measurements for Evaluating Dynamic Physical Properties of a Powder Bed," *Powder Technol.*, **77**, 39 (1993).
Okudaira, Y., H. Ando, M. Satoh, and K. Miyanami, "Dynamic Measurements for the Stiffness Constant of a Powder Bed," *Powder Technol.*, **81**, 139 (1994).
Okudaira, Y., "A Fundamental Study of Sound Absorption in Powders," PhD Thesis, Osaka Prefecture Univ., Osaka, Japan (1997).
Richardson, J., A. J. Matchett, J. M. Coulthard, S. Gibbon, C. Wilson, and C. Watson, "The Characterization of Pigment Powders for Titanium Dioxide/Polymer Dispersions by the 'Masterbatch' Process," *Chem. Eng. Res. Des.*, **78**(Pt. A), 39 (2000).
Shinohara, K., M. Oida, and B. Golman, "Effect of Particle Shape on Angle of Internal Friction by Triaxial Compression Test," *Powder Technol.*, **107**, 131 (2000).
Trappe, V., and D. A. Weitz, "Scaling of the Viscoelasticity of Weakly Attractive Particles," *Phys. Rev. Lett.*, **85**, 449 (2000).
Trappe, V., V. Prasad, L. Cipelletti, P. N. Segre, and D. A. Weitz, "Jamming Phase Diagram for Attractive Particles," *Nature*, **411**, 772 (2001).
Waterman, N. A., and M. F. Ashby, Eds., *The Material Selector*, Vol. 3, 2nd ed., Chapman & Hall, New York (1997).
Yanagida, T., A. J. Matchett, and J. M. Coulthard, "Dissipation Energy of Powder Beds Subject to Vibration," *Chem. Eng. Res. Des.*, **78**(Pt. A), 655 (2001a).
Yanagida, T., A. J. Matchett, and J. M. Coulthard, "Energy Dissipation of Binary Powder Mixtures Subject to Vibration," *Adv. Powder Technol.*, **12**, 227 (2001b).
Yanagida, T., A. J. Matchett, and J. M. Coulthard, "Vibration in Systems of Binary Powder Mixtures—Elastic and Damping Properties and Their Dependence Upon Mixing Quality," *PARTEC 2001*, CD-ROM (2001c).
Yanagida, T., A. J. Matchett, and J. M. Coulthard, "Damping and Elastic Properties of Binary Powder Mixtures," *Powders Grains 2001*, 93 (2001d).
Yanagida, T., A. J. Matchett, and J. M. Coulthard, "Effective Mass of Powder Beds Subjected to Low—Magnitude Vibration and Its Application to Binary Systems, Part 1, Experimental Methodology," *Chem. Eng. Sci.*, **57**, 2653 (2002a).
Yanagida, T., A. J. Matchett, and J. M. Coulthard, "Effective Mass of Powder Beds Subjected to Low—Magnitude Vibration and Its Application to Binary Systems, Part 2, Comparison of Segregated and Well-Mixed Binary Powder Mixtures," *Chem. Eng. Sci.*, **57**, 2663 (2002b).
Yanagida, T., A. J. Matchett, J. M. Coulthard, B. N. Asmar, P. A. Langston, and J. K. Walters, "Dynamic Measurement for the Stiffness of Loosely Packed Powder Beds," *AIChE J.*, **48**, 2510 (2002c).

Appendix: Effective Mass of Horizontally Segregated Systems

In the same manner as Rayleigh's energy method, the shape of the amplitude in each phase is expressed as a linear function of distance

$$z_1 = \left(\frac{z_0 - z_{12}}{h_1}\right) y_1 + z_{12} \tag{A1}$$

$$z_2 = \frac{z_{12}}{h_2} y_2 \tag{A2}$$

where h_1 is the height of upper phase 1, h_2 is the height of lower phase 2, y_1 is the distance from the interface between phases 1 and 2, y_2 is the distance from the fixed end, z_0 is the amplitude of the top end of phase 1, z_1 is the amplitude of any cross section of phase 1, z_2 is the amplitude of any cross section of phase 2, and z_{12} is the amplitude at the interface between phases.

Since the natural circular frequency, ω_n, of each cross section of the phases is the same, the maximum velocities of any cross section along the phases are simply

$$\dot{z}_1 = \left[\left(\frac{z_0 - z_{12}}{h_1}\right) y_1 + z_{12}\right] \omega_n \tag{A3}$$

$$\dot{z}_2 = \left(\frac{z_{12}}{h_2} y_2\right) \omega_n \tag{A4}$$

The maximum kinetic energy $T_{\max}$ of the system used is given by

$$T_{\max} = \frac{1}{2}\rho_1 A \int_0^{h_1} (\dot{z}_1)^2 dy_1 + \frac{1}{2}\rho_2 A \int_0^{h_2} (\dot{z}_2)^2 dy_2 \tag{A5}$$

where ρ_1 and ρ_2 are the densities of phase 1 and phase 2, respectively, and A is the cross-sectional area of the phase.

Substitution of Eqs. A3 and A4 into Eq. A5 gives

$$T_{\max} = \frac{1}{2}\rho_1 A h_1 (\omega_n)^2 \left\{\frac{(z_0 - z_{12})^2}{3} + z_{12}(z_0 - z_{12}) + (z_{12})^2\right\} + \frac{1}{2}\rho_2 A h_2 (\omega_n)^2 \left\{\frac{(z_{12})^2}{3}\right\} \tag{A6}$$

Here, ρAh is equal to the mass of the phase, and the ratio α of z_{12} to z_0 ($z_{12} = \alpha z_0$) is defined.

Equation A6 can be rewritten as follows

$$T_{\max} = \frac{1}{2} m_{p1} (z_0 \omega_n)^2 \left\{\frac{(1-\alpha)^2}{3} + \alpha(1-\alpha) + (\alpha)^2\right\} + \frac{1}{2} m_{p2} (z_0 \omega_n)^2 \left\{\frac{(\alpha)^2}{3}\right\} \tag{A7}$$

Simplifying

$$T_{\max} = \frac{1}{2}(z_0 \omega_n)^2 \left[\frac{m_{p1}}{3}(\alpha^2 + \alpha + 1) + \frac{m_{p2}}{3}(\alpha^2)\right] \tag{A8}$$

The mass term in Eq. A8 corresponds to the effective mass of the segregated binary powder systems, m_1

$$m_1 = \frac{m_{p1}}{3}(\alpha^2 + \alpha + 1) + \frac{m_{p2}}{3}(\alpha^2) \tag{A9}$$

Calculation of m_1 requires the value of α. Here, in order to deduce α from the properties of each phase, we assume that the damping force is negligible compared to the stiffness force.

From the force balance of each phase

$$k_1(z_0 - z_{12}) = k_2 z_{12} \tag{A10}$$

Equation A10 can be given in terms of α, as follows

$$k_1(1-\alpha) = k_2\alpha \tag{A11}$$

Therefore

$$\alpha = \frac{k_1}{k_1 + k_2} \tag{A12}$$

The stiffness is dependent upon the bed height, and is given by

$$k = Y\frac{A}{h} \tag{A13}$$

where Y is Young's modulus of powder bed.

Substituting Eq. A13 into Eq. A12 gives

$$\alpha = \frac{Y_1 h_2}{Y_1 h_2 + Y_2 h_1} \tag{A14}$$

Manuscript received July 11, 2002, and revision received Feb. 24, 2003.